Thermochimica Acta 345 (2000) 157–164

thermochimica acta

www.elsevier.com/locate/tca

The use of MoO_3 and NiO (pure or mixed) oxide catalysts in the decomposition of $KMnO_4$

Samih A. Halawy[a,*], Mohamed A. Mohamed[b]

[a]*Chemistry Department, College of Education, King Faisal University, PO Box 1759, Hufof 31982 Eastern Province, Saudi Arabia*
[b]*Chemistry Department, Faculty of Science, South Valley University, Qena 83511, Egypt*

Received 2 June 1999; received in revised form 8 September 1999; accepted 28 September 1999

Abstract

Non-isothermal decomposition of pure or mixed $KMnO_4$ with (10% w/w) MoO_3 and NiO as well as mixtures of the two oxides was studied using thermogravimetric (TG) and derivative thermogravimetric (DTG) analyses. The catalysts calcined at 500°C were characterized by XRD and IR analyses. The surface area (S_{BET}) of these catalysts were, also, determined. XRD analysis was used to identify the intermediate compounds resulting during the first stage of decomposition of $KMnO_4$, as pure or mixed with some selected catalysts, and the final products of the decomposition at 400°C. A reaction scheme has been proposed to illustrate the decomposition steps of $KMnO_4$. © 2000 Elsevier Science B.V. All rights reserved.

Keywords: Decomposition; $KMnO_4$; MoO_3; NiO; Reaction scheme

1. Introduction

The decomposition of alkali metal permanganates is considered a very interesting subject for investigation. The thermal decomposition of $KMnO_4$, among the alkali metal permanganates, has received relatively more attention by the solid state researchers [1]. Herbstein et al. [2] have studied the first stage of the decomposition of $KMnO_4$ (i.e. up to 300°C). Also, a recently published article [3] described the textures developed during $KMnO_4$ decomposition and have postulated a mechanism of the interface reactions based on nucleation and growth. The influence of pre-irradiation on the kinetics of pyrolysis of $CsMnO_4$ [4] and $RbMnO_4$ [5] has also been studied.

The effect of different additives on the rate of thermal decomposition of $KMnO_4$ has been investigated [6,7] using thermogravimetric (TG) analysis. It was assumed that the most effective catalysts, during the decomposition course of $KMnO_4$, contain holes which significantly accelerate the decomposition of $KMnO_4$ through an electron transfer mechanism [8]. Few articles have been published on the decomposition of other permanganates such as $CsMnO_4$ [4], $RbMnO_4$ [5], $Ni(MnO_4)_2$ [9], $Ba(MnO_4)_2$ [10] and $AgMnO_4$ [11].

In the present study, we have examined the effect of addition of MoO_3, NiO (as pure oxides) and mixtures of both catalyst oxides on the decomposition of $KMnO_4$. The intermediate compounds of the first stage of $KMnO_4$ decomposition and those formed at 280°C together with the final products at 400°C were examined using XRD analysis. A reaction scheme was

---

[*] Corresponding author.
E-mail address: shalawy@kfu.edu.sa (S.A. Halawy).

PII: S0040-6031(99)00363-9

proposed to illustrate the decomposition steps of $KMnO_4$.

2. Experimental

2.1. Preparation of catalysts

Pure MoO_3 and NiO samples were prepared by the direct calcination, at 500°C for 5 h, of analytical grade ammonium molybdate, $(NH_4)_6Mo_7O_{24}\cdot 4H_2O$, and nickel hydroxide [12], $Ni(OH)_2$, respectively. MoO_3 containing 30, 50 and 70 mol% NiO were prepared as follows: calculated amounts of ammonium molybdate and nickel hydroxide were mixed together by deionized water, with vigorous stirring, and the mixture was evaporated to dryness over a water bath. All the resulting mixtures were dried at 120°C in an oven for 12 h. Finally, the catalyst samples were calcined in air at 500°C for 5 h. For simplicity these catalysts are identified here as Cat-30, Cat-50 and Cat-70, respectively.

2.2. Characterization of the catalysts

X-ray powder diffraction (XRD) patterns of the calcined catalysts as well as the decomposition products of $KMnO_4$ as pure or mixed with some selected catalysts, at 280°C and at the end of the pyrolysis, were recorded at ambient temperature. This was carried out using D5000 Siemens diffractometer (Germany), equipped with a copper anode generating Ni-filtered Cu Kα radiation ($\lambda = 1.5406$ Å, 40 kV, 30 mA). An on-line data acquisition and handling system facilitated an automatic JCPDS library search and match (Diffrac. Software, Siemens).

IR absorption spectra of the calcined catalysts were performed using a Perkin-Elmer 599B IR spectrophotometer between 2000 and 200 cm^{-1}, adopting the KBr disc technique.

Surface area (S_{BET}) of all catalysts were measured by the BET method using low-temperature (−196°C) nitrogen adsorption with the aid of a conventional volumetric instrument [13].

2.3. Reactivity measurements

Potassium permanganate (PP) $KMnO_4$ used in this study was an analytical grade material (BDH, UK). Samples of anhydrous PP were crushed gently, before the pyrolysis study, to avoid the effect of particle size variation of the reactants. The crushed $KMnO_4$ were then ground in an agate mortar with 10% w/w of each catalyst and sieved. All these mixtures were stored in a dissector, over anhydrous $CaCl_2$, at ambient temperature. TG of $KMnO_4$, as pure or mixed samples, was carried out using the gasometric technique [14] as explained in detail elsewhere [15].

2.4. Data analysis

The kinetic parameters of the pyrolysis of $KMnO_4$, as pure or mixed with different catalysts, were calculated from the TG results using the Coats–Redfern equation [16] as follows:

$$\log_{10}\left[\frac{1-(1-\alpha)^{(1-n)}}{T^2(1-n)}\right] = \log_{10}\frac{AR}{aE}\left[1-\frac{2RT}{E}\right] - \frac{E}{2.3R}\frac{1}{T} \quad \text{for } n<1,$$

or

$$\log_{10}\left[-\log_{10}\frac{(1-\alpha)}{T^2}\right] = \log_{10}\frac{AR}{aE}\left[1-\frac{2RT}{E}\right] - \frac{E}{2.3R}\frac{1}{T} \quad \text{for } n=1,$$

where α is the fractional mass loss (calculated from TG results), n the reaction order, A the frequency factor, a the heating rate, R the gas constant and T the absolute temperature (K). Using values of (n) equal to 0.25, 0.5, 0.75 and 1.0, in the above mentioned equations, for a given set of experimental values of α and T plots of $\log_{10}[1-(1-\alpha)^{1-n}/T^2(1-n)]$ or $\log_{10}[-\log_{10}(1-\alpha)/T^2]$ against $1/T$ were constructed. The value of n that has given the best fit was chosen as a reaction order and from the slope of that line E_a (kJ/mol) was calculated [17].

3. Results and discussion

3.1. X-ray diffraction analysis

XRD diffractograms of the prepared catalysts, calcined at 500°C for 5 h, are presented in Fig. 1. Diffractogram (a) of the parent MoO_3 matches well

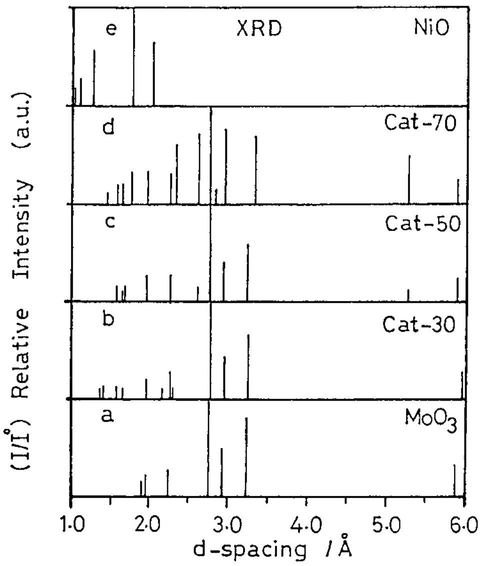

Fig. 1. (a) XRD patterns of MoO_3; (b–d) MoO_3 mixed with 30, 50 and 70 mol% NiO; and (e) NiO calcined at 500°C for 5 h.

the standard ICDD card No. 5-0508, where the most intense peaks appeared at $d = 5.87$, 3.22, 2.92, 2.75, 2.24, 1.95 and 1.92 Å. Diffractogram (b) shows the effect of the addition of 30 mol% NiO to MoO_3 (Cat-30). New lines appear that were attributed to the formation of the following two new phases: (i) $NiMoO_4$ confirmed by the diffraction lines at $d = 1.65$ and 1.57 Å (ICDD card No. 16-0291) and (ii) Ni_2O_3 confirmed by three diffraction lines at $d = 2.29$, 2.15 and 1.36 Å (ICDD card No. 14-0481). The other diffraction lines appearing in pattern (b), i.e. at $d = 5.99$, 3.25, 2.95, 2.78, 2.26, 1.96 and 1.40 Å belong to the parent compound.

XRD pattern (c) of Cat-50 showed the appearance of four new diffraction lines at $d = 5.28$, 2.62, 1.65 and 1.57 Å. These were attributed to the formation of $NiMoO_4$ (ICDD card No. 16-0291), while the other group of diffraction lines at $d = 5.91, 3.22, 2.93, 2.76$, 2.25, 1.95 and 1.68 Å belong to MoO_3 as a main constituent of this. Diffractogram (d) of Cat-70, MoO_3 containing 70 mol% NiO, showed that nickel molybdate has been considerably formed as concluded from the new diffraction lines appearing at $d = 5.28$, 3.33, 2.82, 2.62, 2.32, 1.63 and 1.57 Å which is consistent with ICDD card No. 16-0291. A single diffraction line at $d = 1.75$ Å is attributed to NiO (ICDD card No. 4-0835). The remaining diffraction lines (i.e. at $d = 5.91, 2.95, 2.77, 2.24, 1.96$ and 1.44 Å are attributed to the parent MoO_3. The XRD pattern of pure NiO calcined at 500°C, Fig. 1e, matches well with the ICDD card data No. 4-0835 (with d-spacing values at $d = 2.04$, 1.76, 1.26, 1.11 and 1.02 Å).

From the XRD data shown in Fig. 1 one can notice that Ni_2O_3 has been formed with the addition of a small concentration of NiO to MoO_3 as in Cat-30 (see Fig. 1b). The formation of $NiMoO_4$, on the other hand, has started in Cat-30 and its concentration increased, gradually, with increasing the mol% of NiO added to MoO_3.

3.2. IR analysis

Fig. 2 shows the IR spectra of the catalysts calcined at 500°C for 5 h. The spectra of MoO_3, Cat-30, Cat-50 and Cat-70 possess the same absorption band at 980–970 cm^{-1} corresponding to Mo=O stretching mode [18], followed by a group of bands in the range 870–805 cm^{-1} which are attributed to the stretching mode

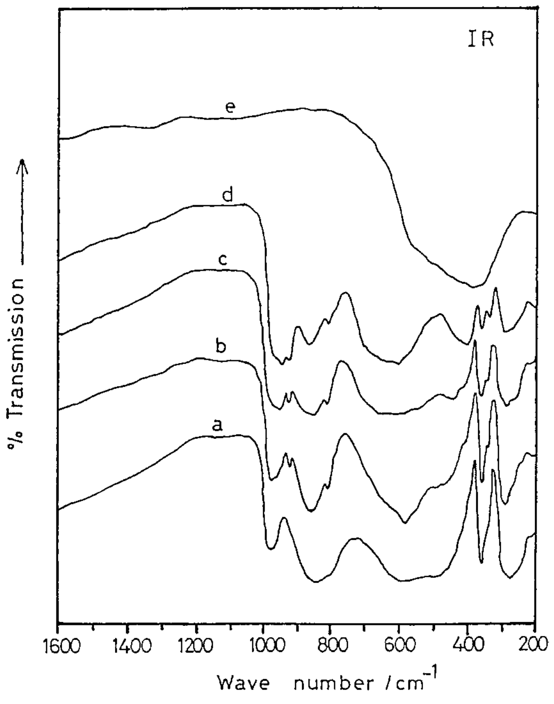

Fig. 2. (a) IR spectra of MoO_3; (b–d) MoO_3 mixed with 30, 50 and 70 mol% NiO; and (e) NiO calcined at 500°C for 5 h.

of the bridge oxygen Mo–O–Mo [19]. The bands due to O–Mo–O deformation mode appeared in the range 500–235 cm^{-1} in spectra (Fig. 2a–d). The IR spectra of samples Cat-30, Cat-50 and Cat-70 showed new bands at 950–920 and 600–440 cm^{-1}, which are related to the formation of $NiMoO_4$ in these catalysts [20]. The spectrum of NiO (Fig. 2e) shows a weak shoulder at 650 cm^{-1} followed by two high intensity broad bands at 450 and 385 cm^{-1}, which are attributed to the stretching vibration of Ni–O [21].

3.3. Reactivity measurements

TG curves of the pyrolysis of $KMnO_4$ (PP), pure or mixed with 10% w/w catalysts, are shown in Fig. 3. The pure PP started to decompose significantly at ≅240°C, the rate of decomposition becomes appreciably fast in the temperature range 265–285°C and slowed down afterwards till 450°C. The derivative thermogravimetric analysis (DTG) curve of pure PP (Fig. 4a) shows that the maximum rate of weight loss as a sharp peak at $T_{max} = 275°C$. The addition of 10% w/w of pure MoO_3 or NiO, that calcined at 500°C, to PP has a notable enhancing effect on the pyrolysis of PP (Fig. 3b and c). This is further indicated by the shift of T_{max} of the DTG curves towards lower temperatures. Both MoO_3 and NiO have an accelerating effect during the decomposition of PP by 14°C (for MoO_3) and 26°C (for NiO) (see Fig. 4b and c). The addition of 10% w/w of Cat-30 has strongly retarded the decomposition of PP (see Fig. 3d). The decomposition step was shifted to 280°C, then, was accelerated between 295°C and 400°C and has been completed at about 500°C. Again, the DTG curve of PP in the presence of Cat-30, Fig. 4d, showed that the T_{max} value was shifted by 45°C higher than the pure PP. Fig. 3 shows the positive effect of addition of 10% w/w of Cat-50 and (curve e) and Cat-70 (curve f) on the decomposition of PP. It is clear that both catalysts have accelerated the decomposition reaction. For example, the presence of Cat-70 (curve f), the decomposition reaction commenced too early with the evolution of considerable amounts of oxygen and the rate has increased appreciably between 220°C and 450°C. Fig. 4e and f, further supports the accelerating effect of both Cat-50 and Cat-70 on the decomposition of PP where T_{max} are maximized at 247°C and 240°C, respectively.

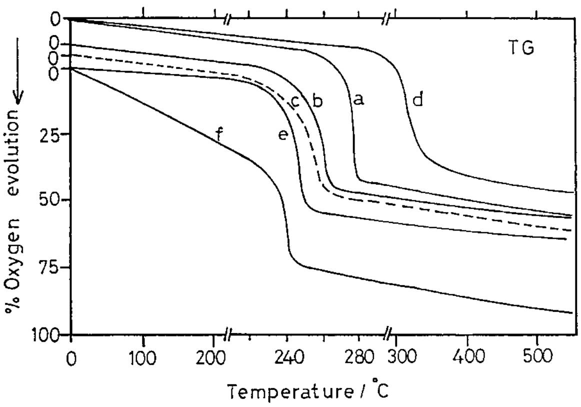

Fig. 3. TG curves of the pyrolysis of: (a) $KMnO_4$ (PP), PP mixed with 10% w/w of the respective catalysts, calcined at 500°C, (b) MoO_3, (c) NiO, (d) Cat-30, (e) Cat-50 and (f) Cat-70.

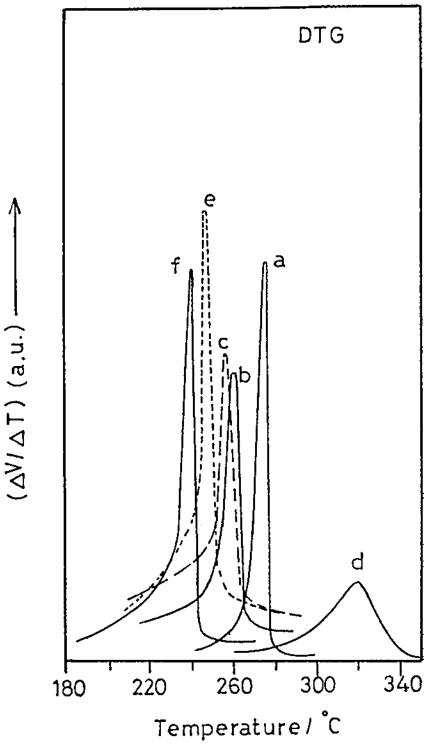

Fig. 4. DTG curves of the pyrolysis of: (a) $KMnO_4$ (PP), PP mixed with 10% w/w of the respective catalysts, calcined at 500°C, (b) MoO_3, (c) NiO, (d) Cat-30, (e) Cat-50 and (f) Cat-70.

From the TG and DTG results, it is seen that addition of the pure oxides (i.e. MoO_3 or NiO) has accelerated the decomposition of PP. This is explained by the fact that $KMnO_4$ is an n-type semiconductor [8] which is reported [8] to decompose via an electron transfer mechanism. Therefore, typical p-type semiconductors [22] such as MoO_3 and NiO which act well as an electron acceptor are expected to enhance the decomposition of $KMnO_4$. The addition of 10% w/w of Cat-30 to $KMnO_4$, on the other hand, has retarded the decomposition process (see Fig. 3d and Fig. 4d). This behaviour could be attributed to the formation of the n-type semiconductor Ni_2O_3 [22] on calcination of this sample at 500°C, see the XRD results. Therefore, the presence of a minute concentration of Ni_2O_3 which acts as an electron donor will strongly inhibit the decomposition of $KMnO_4$. As the mol% of NiO added to MoO_3 increases, i.e. 50 and 70 mol%, the concentration of $NiMoO_4$ formed increases. Therefore, Cat-70, containing 70 mol% NiO, was the most active catalyst for the decomposition of $KMnO_4$ among the catalysts investigated.

3.4. Reaction stoichiometry

The decomposition of $KMnO_4$ up to 300°C was reported to proceed by the following equation [2]:

$$10KMnO_4 \rightarrow 2.65K_2MnO_4 + [2.35K_2O \cdot 7.35MnO_{2.05}] + 6O_2 \quad (1)$$

Boldyrev et al. [23] have identified both $K_3(MnO_4)_2$ and K_2MnO_4 as intermediates during the decomposition of $KMnO_4$. Therefore, we can assume that the decomposition of $KMnO_4$ may proceed via the following equations:

$$3KMnO_4 \rightarrow K_3(MnO_4)_2 + MnO_2 + O_2 \quad (2)$$

$$2K_3(MnO_4)_2 \rightarrow 2K_2MnO_4 + K_2O + 2MnO_2 + 1.5O_2 \quad (3)$$

$$2K_2MnO_4 \rightarrow 2KMnO_2 + K_2O + 1.5O_2 \quad (4)$$

The summation of the last three equations gives the overall reaction scheme:

$$6KMnO_4 \rightarrow 2KMnO_2 + 2K_2O + 4MnO_2 + 5O_2 \quad (5)$$

To prove the above mentioned assumption, we have carried out the decomposition of $KMnO_4$ (pure or catalyzed) up to 280°C. The solid product (at 280°C) was transferred into a desiccator containing anhydrous $CaCl_2$, left to cool and was finally subjected to XRD analysis. Similarly, the final decomposition product at 400°C was subjected to XRD analysis. The XRD results of these decomposition products of $KMnO_4$ (pure or catalyzed), at 280°C and 400°C are given in Table 1. The XRD results listed in Table 1 show the presence of the reaction intermediates mentioned above (Eqs. (2)–(5)), i.e. $K_3(MnO_4)_2$, K_2MnO_4, $KMnO_2$and $K_2Mn_2O_3$. In addition, another intermediate (i.e. $K_2Mn_4O_3$) was identified in all samples (except for PP + MoO_3) decomposed up to 280°C. δ-MnO_2 was identified in the reaction products of all samples investigated, while ξ-MnO_2 and K_2O were identified only after decomposition to 400°C.

3.5. Kinetic analysis

The activation energy E_a for the decomposition of $KMnO_4$ (PP) pure or mixed with, 10% w/w, different catalysts was calculated using the Coats–Redfern equation [16], and the results are given in Table 2. The value of E_a calculated for pure PP was 151 kJ mol^{-1}. This value is in good agreement with that reported before [24,25]. The addition of the pure oxides, i.e. MoO_3 and NiO, to PP has resulted in a decrease of E_a to 125.8 and 127.3 kJ mol^{-1}, respectively. The same effect was observed on the addition of Cat-50 or Cat-70 during the decomposition of PP(see Table 2). On the contrary, the value of E_a of the decomposition of PP mixed with Cat-30 was increased to 160.3 kJ mol^{-1}, which is attributed to the retardation effect of Ni_2O_3 thus formed during the preparation of Cat-30 at 500°C, see the XRD analysis. From the kinetic results of the non-isothermal decomposition of PP (Table 2), it is clear that the catalytic activity of these catalysts have been affected by their chemical composition. For example, increasing the concentration of the p-type $NiMoO_4$ [26] formed during their preparation, e.g. Cat-70 has increased its activities (see the XRD results and Table 2). On the other hand, the formation of the n-type semiconductor Ni_2O_3 [22], e.g. Cat-30, has resulted in a decrease in its activity (see XRD results and Table 2). It is worth mentioning here that S_{BET} of these catalysts did not play an important role in the present study except, to some extent, for Cat-70 which possessed the highest S_{BET} value (i.e. 36.1 m^2 g^{-1}).

Table 1
XRD results of the decomposition of $KMnO_4$ as self or mixed with MoO_3, NiO and Cat-50 at 280°C and the final products at 400°C[a]

Identification of the products by the standard ICDD data	Step (I) at 280°C				Step (II) at 400°C			
	$KMnO_4$ (PP)	PP + MoO_3	PP + NiO	PP + Cat-50	$KMnO_4$ (PP)	PP + MoO_3	PP + NiO	PP + Cat-50
$KMnO_4$ ICDD card No. (7-0023)	4.595 3.914 3.437 1.936 1.806 1.702	3.705 3.206 2.957 2.847 2.205 1.729	5.749 3.880 3.437 3.218 2.947 2.562 1.916 1.836 1.671	3.559 3.229 2.820 1.916 1.809 1.596	1.936 1.806 1.700	3.705 3.386 3.218 2.938 2.199 1.700	4.572 3.573 3.437 2.938 2.855 1.660	1.916
$K_3(MnO_4)_2$ ICDD card No. (21-0997)	3.241 2.882 2.384 1.773 1.745	3.645 1.971 1.767	4.844 3.252 2.882 2.421 1.959	3.264 1.963 1.779	1.748	2.453 1.975 1.796	4.870 1.641 1.596	2.415 1.975 1.786 1.627
K_2MnO_4 ICDD card No. (12-0264)	4.247 3.815 3.601 3.066 2.976 2.938 2.285 2.144	3.798 2.920 2.144 2.065	5.122 3.799 3.076 2.590 2.473 2.274 2.154 2.034 1.897	3.151 3.119 3.076 2.976 2.144 2.056	4.247 3.831 3.056 2.976 2.928	3.815 3.587 3.097 2.976 2.910 2.130	5.122 4.308 4.247 3.815 3.076 2.576 2.279 2.460	4.247 3.816 3.151 3.076 2.976 2.285 2.130 2.039
$KMnO_2$ ICDD card No. (18-1035)	2.778 2.263	7.132 3.517 2.409	7.076 3.545 2.769 2.125 2.061	7.076 2.130 2.120	7.020 2.769	7.132 3.517 2.402	7.076	7.020
$K_2Mn_2O_3$ ICDD card No. (38-1062)	2.736 2.539		2.728 2.657	2.891 2.650 2.506	2.728	2.547	2.761	2.720
$K_2Mn_4O_3$ ICDD card No. (16-0205)	6.965 3.490		6.965 3.504	3.463				
δ-MnO_2 ICDD card No. (14-0644)	3.966 2.319 2.125 1.609 1.306	3.966 2.434 1.646 1.520	2.319 1.633 1.301 1.233	1.480 1.420 1.386	2.336 2.125 1.619 1.509 1.420 1.383 1.243	2.612 2.434 2.092 1.657	2.409 1.244	2.605 1.607 1.251
ξ-MnO_2 ICDD card No. (12-0141)					2.460 2.384 2.135 2.061 1.959 1.677	3.880 2.479 2.258 2.039	1.677	

Table 1 (*Continued*)

Identification of the products by the standard ICDD data	Step (I) at 280°C				Step (II) at 400°C			
	$KMnO_4$ (PP)	PP + MoO_3	PP + NiO	PP + Cat-50	$KMnO_4$ (PP)	PP + MoO_3	PP + NiO	PP + Cat-50
K_2O ICDD card No. (23-0493)					3.705 2.313 2.279 1.897 1.799 1.768	2.285 1.872	2.263	

[a] All XRD lines, in this table, have highly relative intensities.

Table 2
Kinetic results of the non-isothermal decomposition of pure $KMnO_4$ (PP) and PP mixed with 10% w/w catalysts and the S_{BET} values of these catalysts, calcined at 500°C for 5 h

Sample	T_{max} (DTG) (°C)	E_a (kJ/mol)	n^a	Coresponding coefficient	S_{BET} (m^2/g)
$KMnO_4$ (PP)	275	151.0	0.25	0.97	–
PP + MoO_3	261	125.8	1.00	0.96	$MoO_3 = 1.3$
PP + NiO	249	127.3	0.25	0.98	NiO = 34.1
PP + (Cat-30)	320	160.3	0.25	0.99	Cat-30 = 22.9
PP + (Cat-50)	247	109.5	0.25	0.98	Cat-50 = 18.6
PP + (Cat-70)	240	92.0	1.00	0.94	Cat-70 = 36.1

[a] Order of reaction.

Acknowledgements

Mr. E.A. El-Katatny, Aluminium Company of Egypt, Nag-Hammady, Egypt, is thanked for performing the XRD analysis.

References

[1] M.E. Brown, D. Dollimore, A.K. Galwey, Comprehensive Chemical Kinetics, vol. 22, Elsevier, Amsterdam, 1980.

[2] F.H. Herbstein, G. Ron, A. Weissman, J. Chem. Soc. A, (1970) 1821.

[3] M.E. Brown, A.K. Galwey, M.A. Mohamed, H. Tanaka, Thermochim. Acta 235 (1994) 255.

[4] A.K. Galwey, S.A.A. Mansour, Thermochim. Acta 228 (1993) 379.

[5] P.J. Herley, E.G. Prout, J. Inorg. Nucl. Chem. 16 (1960) 16.

[6] J.S. Booth, D. Dollimore, G.R. Heal, Thermochim. Acta 39 (1980) 293.

[7] A.A. Said, K.M. Abd El-Salaam, E.A. Hassan, Surf. Technol. 19 (1983) 241.

[8] V.V. Boldyrev, Phys. Chem. Solids 30 (1969) 1215.

[9] A.K. Galwey, S.A.A. Fakiha, K.M. Abd El-Salaam, Thermochim. Acta 206 (1992) 297.

[10] E.G. Prout, Herley, J. Phys. Chem. 65 (1961) 208.

[11] E.G. Prout, F.C. Tompkins, Trans. Faraday Soc. 42 (1946) 468.

[12] S.T. Teichner, J.A. Morrison, Trans. Faraday Soc. 51 (1955) 961.

[13] B.C. Lippens, J.H. de Boer, J. Catal. 4 (1965) 319.

[14] A.I. Onuchukwa, P.B. Mshelia, J. Chem. Educ. 62 (1985) 809.

[15] S.A. Halawy, J. Anal. Appl. Pyrolysis 38 (1996) 89.

[16] J.W. Coats, J.P. Redfern, Nature (London) 201 (1964) 58 and 101.

[17] S.A. Halawy, M.A. Mohamed, Collet. Czech. Chem. Commun. 59 (1994) 2253.

[18] M. Niwa, M. Kizutani, M. Takahashi, Y. Murakami, J. Catal. 70 (1981) 14.

[19] F. Trifiro, S. Notarbartolo, I. Pasquon, J. Catal. 22 (1971) 324.

[20] P.P. Cord, P. Courtine, G. Pannetier, J. Guillermet, Spectrochim. Acta A 28 (1972) 1601.

[21] J.R. Ferraro, Low-frequency Vibrations of Inorganic and Coordination Compounds, Plenum Press, New York, 1974, p. 74.
[22] O.V. Krylov, Catalysis by Non-metals, Academic Press, New York, 1970, p. 254.
[23] V.V. Boldyrev, Z.G. Vinokurova, L.N. Senchenko, B.G. Erenburg, Zh. Neorg. Khim. 15 (1970) 9.
[24] M.E. Brown, K.C. Sole, M.W. Beck, Thermochim. Acta 92 (1985) 149.
[25] R.A.W. Hill, R.T. Richardson, B.W. Rodger, Proc. R. Soc. London. Ser. A 291 (1966) 208.
[26] Z.G. Szabó, D. Kalló, Contact Catalysis, vol. 1, Elsevier, Amsterdam, 1976.